

Original Research

Effects of solidification cooling rate on the corrosion resistance of Mg–Zn–Ca alloy

Debao Liu^{a,*}, Yichi Liu^a, Yan Huang^b, Rong Song^a, Minfang Chen^a

^a*School of Materials Science and Engineering, Tianjin University of Technology, Tianjin 300384, China*

^b*BCAST, Brunel University, Uxbridge, Middlesex UB8 3PH, UK*

Received 2 July 2014; accepted 1 September 2014

Available online 29 October 2014

Abstract

This study was carried out to investigate the effect of solidification cooling rate on the corrosion resistance of an Mg–Zn–Ca alloy developed for biomedical applications. A wedge shaped copper mould was used to obtain different solidification cooling rates. Electrochemical and immersion tests were employed to measure the corrosion resistance of Mg–Zn–Ca alloy. It was found that increasing cooling rate resulted in a significant improvement in the corrosion resistance of the Mg–Zn–Ca alloy. The findings were explained in terms of solidification behaviour in association with the change in solubility of the alloying elements, microstructural homogeneity and refinement and chemical homogeneity as well as the increased cooling rates.

© 2014 Chinese Materials Research Society. Production and hosting by Elsevier B.V. All rights reserved.

Keywords: Mg–Zn–Ca alloy; Solidification cooling rate; Microstructure; Corrosion resistance

1. Introduction

Magnesium alloys are potential candidates for degradable load-bearing implant materials due to their excellent biocompatibility, degradability and osteoconductivity. The major drawback of magnesium alloys serving as implant materials at present is their poor corrosion resistance in physiological environment, and thereby they lose their mechanical integrity before tissues have sufficiently healed [1]. The corrosion rate of magnesium can be improved in various ways, mainly by surface coating and alloying [2]. For example, Mg alloys containing Zn and Ca elements have attracted much attention as orthopaedic biomaterials in recent years. Zn and Ca are chosen as alloying elements for magnesium alloy as orthopaedic biomaterials due to several reasons. Firstly, Zn and Ca are essential elements for the human body. Secondly, Ca is a major component of the human bone and can accelerate

bone growth in implantation. Thirdly, a suitable amount of Zn and Ca can improve both the corrosion resistance and mechanical properties of magnesium alloys, which is mainly realized by grain refinement [3–11]. Therefore, Mg–Zn–Ca alloys for degradable bone internal fixation has been studied in recent years [12,13]. Besides the surface coating and alloying, microstructural refinement of magnesium can lead to a significant improvement in the corrosion resistance due to the alteration of passive layer characteristics [14–17]. Relevant research shows that grain refinement by means of plastic deformation can improve the corrosion resistance of magnesium alloy [18–20]. Moreover, solidification rate has been found to have a strong impact on grain refinement and therefore the corrosion behaviour of magnesium alloy [21–24]. However, there is a lack of research on the effect of solidification rate on corrosion resistance of Mg–Zn–Ca magnesium alloys, which limits the development of the material. In this study, Mg–Zn–Ca alloys with different grain sizes were prepared by the cooling rate-controlled solidification to investigate the influence of grain size on corrosion behaviour in simulated body fluid.

*Corresponding author. Tel.: +86 22 60214008; fax: +86 22 60214028.

E-mail address: debaoliu@126.com (D. Liu).

Peer review under responsibility of Chinese Materials Research Society.

2. Material and experimental method

Pure Mg ingot was melted at 720 °C under the protection of a gas mixture containing SF₆ and N₂. Calculated amounts of pure Zn and Mg–45%Ca master alloy were added to the Mg melt and then held for 30 min to ensure that Zn and Mg–Ca master alloy gets melted and diffuses sufficiently. The melt was cast into a wedge shaped copper mould, at different cooling rates, to obtain an Mg–2Zn–0.5Ca (all in wt%) alloy with different grain sizes. Fig. 1 shows the wedge shape copper mould. The cooling rate was controlled by adjusting the dimensions of the mould using an empirical relationship between the cooling rate (T in K s^{-1}) and the half thickness of the wedge (z in mm), i.e., the distance from the walls to the central axis of the mould [25]

$$T = k \cdot zn \quad (1)$$

where k and n are constants. For Cu, k is estimated to be 400 W/mK. The cooling rate at the tip of the mould is approximately 1000 K s^{-1} . The cooling rate as a function of the mould height was measured by recording the cooling curves at various points along the wedge using thermocouples. Five samples for microstructural examinations and other analyses were cut from different locations in the wedge shaped Mg–2Zn–0.5Ca ingot as shown in Fig. 1 and labelled as C_1 to C_5 .

Microstructural observations were performed on an optical microscope (OM, Zeiss AX10) and phase constitutions were characterized by X-ray diffraction (XRD, Rigaku D/max/2500PC). Potentiodynamic polarization and electrochemical impedance spectroscopy (EIS) experiments were performed in a three-electrode cell, using a platinum foil as the counter electrode and an Ag/AgCl (saturated KCl) electrode as the reference electrode, using a Zahner Zennium electrochemical workstation. Immersion tests were performed, following ASTM-G31-72, in an SBF (pH 7.4) at 37 °C in a WE-3 immersion oscillator. Samples were removed after 3 days of the immersion, rinsed with distilled water and dried at room temperature. Then the surface morphology after the immersion was observed using scanning electron microscopy (SEM, JSM-6700F). The weight loss of the immersed samples were measured after removing the corrosion products with a chromic acid and the degradation rates were obtained according to the following equation [26]:

$$\text{Corrosion rate} = (K \times W)/(A \times t \times D) \quad (2)$$

where the coefficient $K=8.76$, W is the weight loss (g), A is the sample area exposed to the solution (cm^2), t is the exposure time (h) and D is the density of the material (g/cm^3).

3. Results and discussion

3.1. Microstructure and phase constitutes at different cooling rates

Fig. 2 shows a typical microstructure of the Mg–2Zn–0.5Ca alloy solidified at different cooling rates. It is clear from the figure that the average grain size for the alloy decreases with

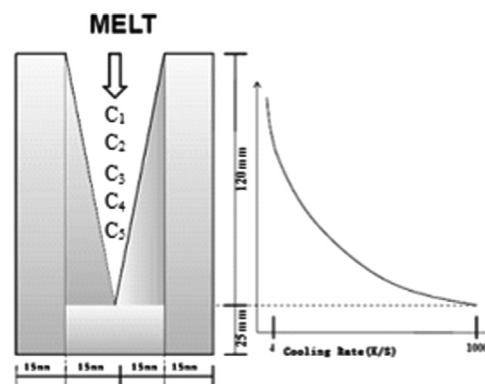


Fig. 1. Schematic illustration of the Cu wedge mould, showing the dimensions and typical cooling rate as a function of height of the mould.

increasing solidification rate. The average grain size was measured from the micrographs using the mean linear intercept method, to be 165 μm , 120 μm , 80 μm , 45 μm and 15 μm . The high magnification images of C1 and C4 are shown in Fig. 3. It can be seen that the Mg–2Zn–0.5Ca alloy is mainly consisted of the primary α -Mg phase and secondary phases, which is along the grain boundary. It also can be seen from Fig. 3 that as solidification rate increases, the eutectic secondary phase structure becomes more dispersive and continuous. Fig. 4(a) is the XRD patterns of the C1 sample. It can be seen that the phases in Mg–2Zn–0.5Ca alloy are primary Mg, $\text{Ca}_2\text{Mg}_6\text{Zn}_3$, Mg_2Ca and MgZn phases. Fig. 4(b) is the EDS spectrums at location by arrow as shown in Fig. 3 (a), which indicate that the secondary phase along the grain boundary in Mg–2Zn–0.5Ca alloy should be ternary compound consisted of Mg, Zn and Ca element. According to the Mg–Zn–Ca ternary phase diagram, the eutectic $\text{Ca}_2\text{Mg}_6\text{Zn}_3$ phase structure forms when the Zn/Ca atomic ratio is higher than 1.2 [27]. Combined with the XRD result, the secondary phase along the grain boundary in Mg–2Zn–0.5Ca alloy should be $\text{Ca}_2\text{Mg}_6\text{Zn}_3$ phase.

3.2. Electrochemical results

The polarization curves from electrochemical tests are shown in Fig. 5(a). It was found that the alloy exhibited higher corrosion potential as the cooling rate increased. Corrosion potential is the combined result of the electrochemical reaction at the interface between sample and the SBF solution. This suggests that the increase in solidification rate decreases susceptibility to electrochemical reaction. Rapid solidification brings about an increase in the solid solubility of zinc and calcium into the magnesium matrix, which is beneficial to form a protected film containing zinc and calcium element on the surface of alloy and this film can protect the alloy to avoid further corrosion [28,8]. Moreover, rapid solidification also brings about an increase in the solid solubility of some impurity elements affecting the corrosion resistance, which would decrease the susceptibility to corrosion.

The Nyquist spectrums for the Mg–2Zn–0.5Ca alloy in Fig. 5(b) show that the capacitive loop enlarges with cooling rate. The diameter of the capacitive semicircle of a Nyquist plot is related to the corrosion rate and an increase in the

diameter represents a decrease in corrosion rate. Fig. 5(b) thus demonstrates clearly the effect of an increased cooling rate on improving corrosion resistance for the material. It can also be seen from the figure that the high frequency region capacitive

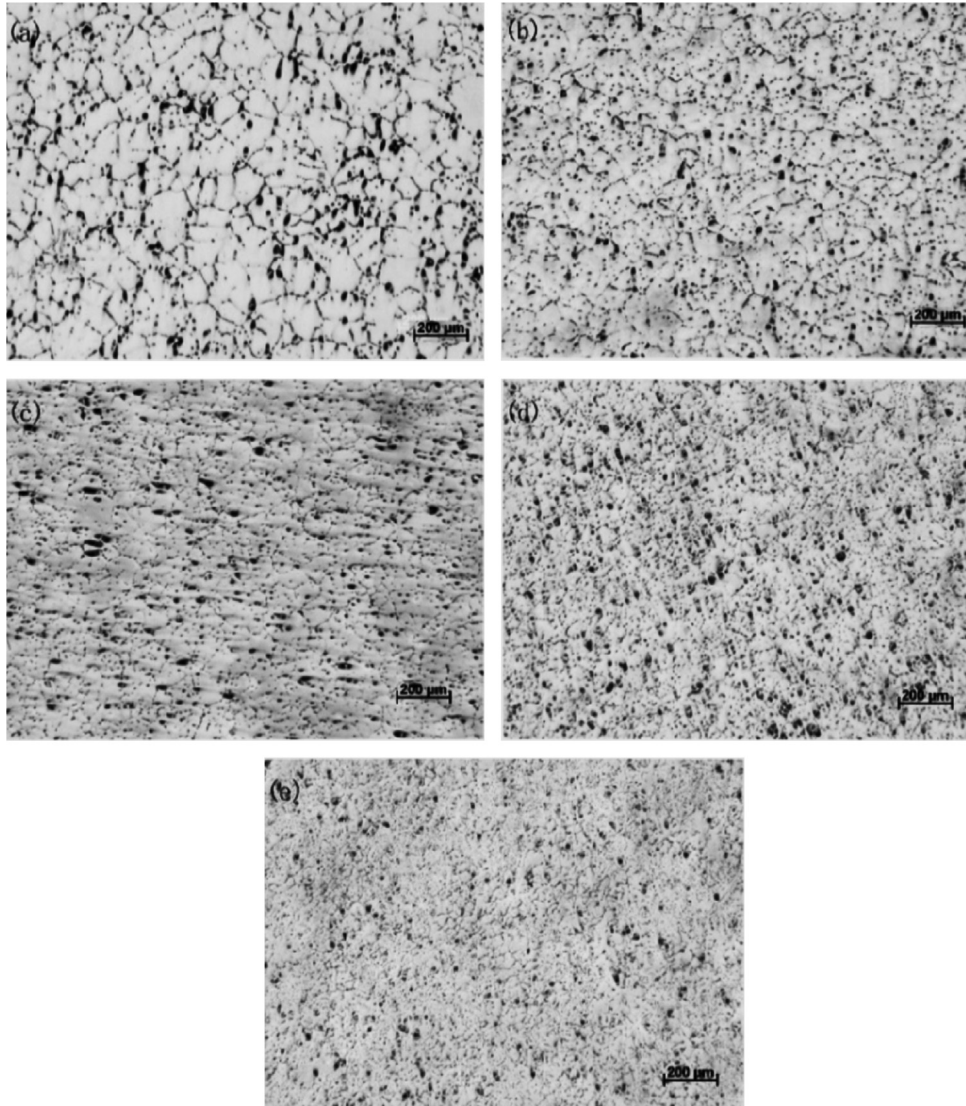


Fig. 2. Microstructures of the Mg–2Zn–0.5Ca alloy with different cooling rates of the samples: (a) C1, (b) C2, (c) C3, (d) C4 and (e) C5.

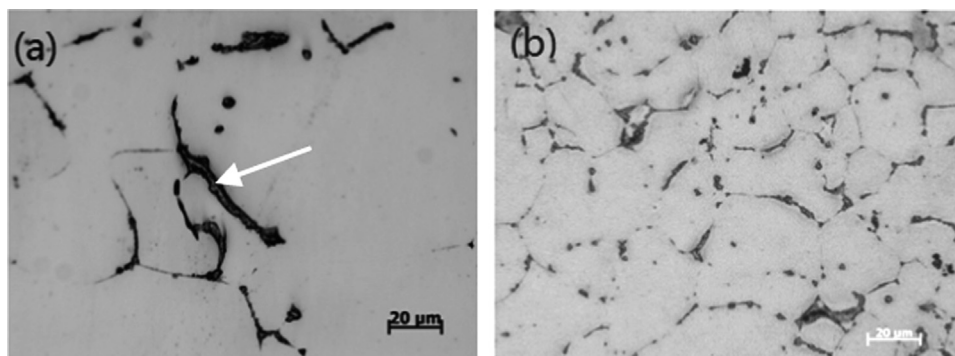


Fig. 3. Variation in distribution and size of the secondary phases with colling rate of the samples: (a) C1 and (b) C4.

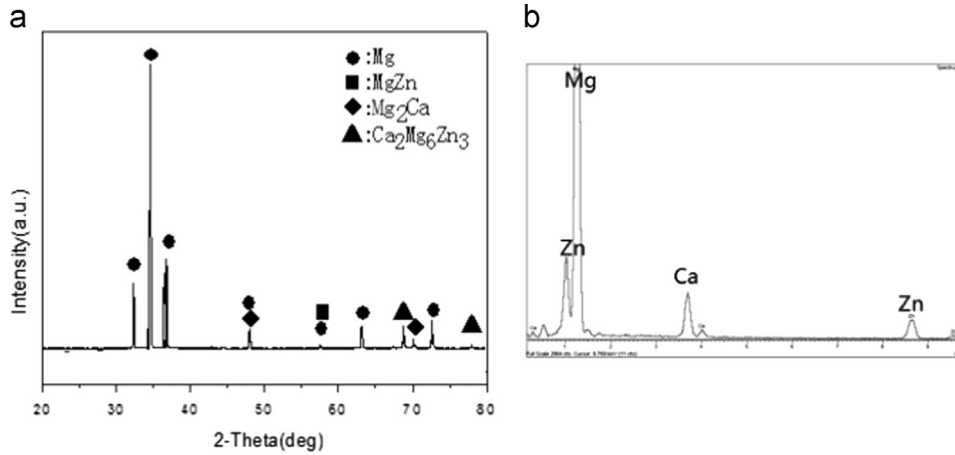


Fig. 4. XRD patterns of C1 sample (a) and EDS spectrums at location by arrow as shown in Fig. 3(a).

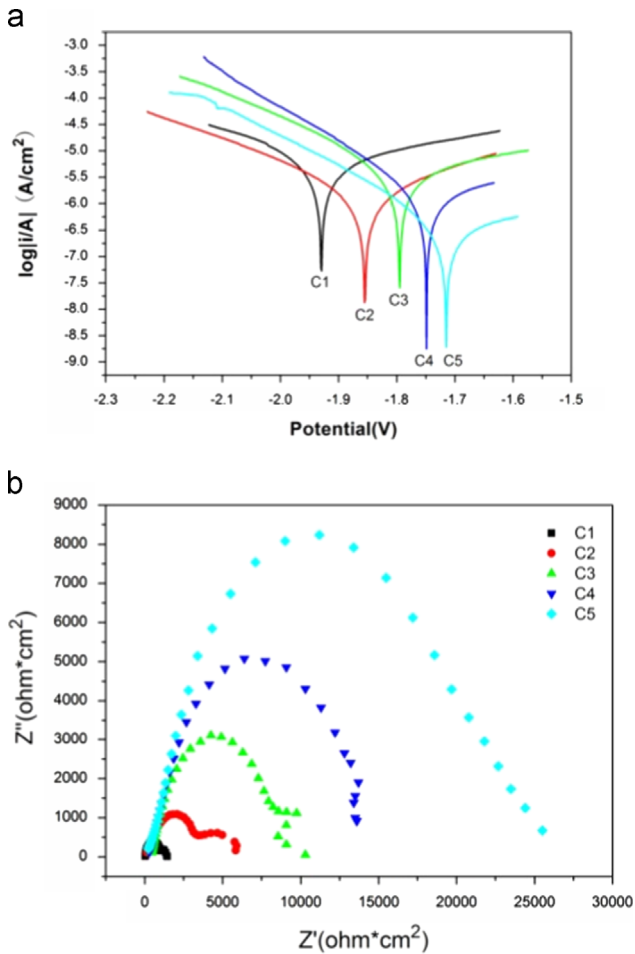


Fig. 5. (a) Polarization curves and (b) EIS of the Mg–2Zn–0.5Ca alloy at different cooling rates.

arc coexists with the middle frequency region capacitive arc in the frequency range of the capacitive loops for the C1–C3 samples. Normally, a high frequency region capacitive arc is caused by charge transfer between electric double layers on the sample surface. This suggests that the corrosion of magnesium

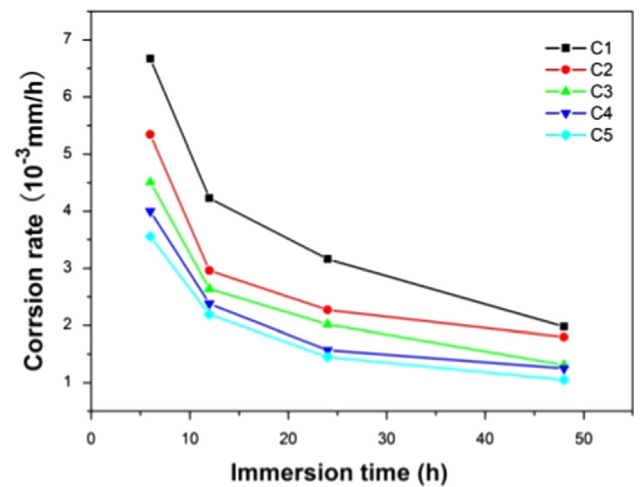


Fig. 6. Corrosion rate of the Mg–2Zn–0.5Ca alloy with different solidification cooling rates immersed in the SBF.

alloy in the SBF involved a charge-transfer-controlled dissolution process, with the formation of a corrosion product film on the surface, and a dissolution process through the film. When a magnesium alloy surface is free of corrosion products or the corrosion film is of a porous nature, the corrosion process is controlled by charge-transfer controlled dissolution and/or diffusion of the reactants for the cathodic reaction. A capacitive arc in medium frequency range is related to the mass transfer process of corrosion products due to the growth of the corrosion product layer. The C1, C2 and C3 samples with relatively larger grain sizes possessed lower corrosion potential so that they tended to get corroded more easily at the initial stage and the corrosion product layer formed readily, causing the middle frequency region capacitive arc as displayed in Fig. 5(b). The C4 and C5 samples showed only high frequency region capacitive arc, indicating that a corrosion product layer was not formed at the initial stage of corrosion due to their higher corrosion potential, therefore the second capacitive arc did not emerge during testing process.

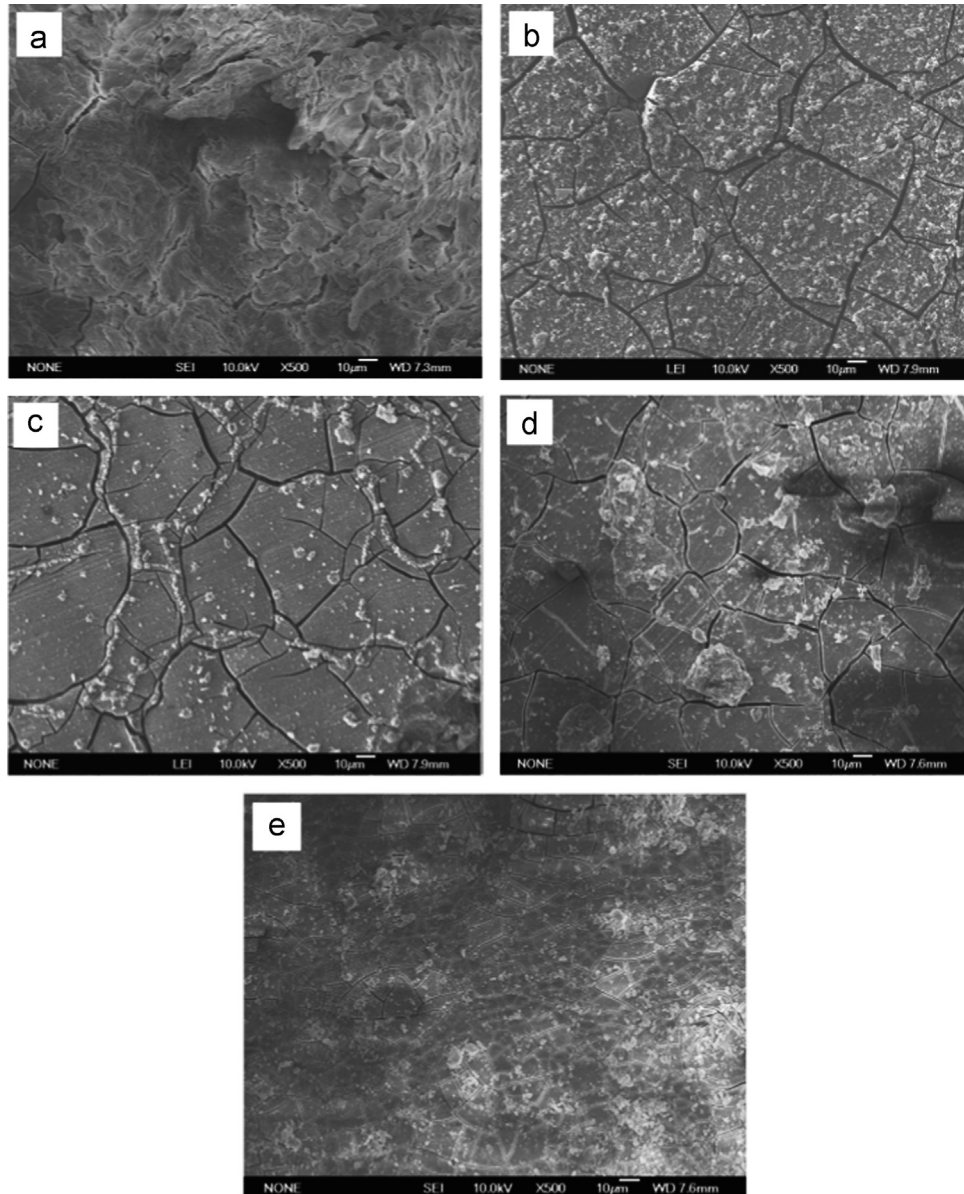


Fig. 7. Surface morphology of Mg–2Zn–0.5Ca alloy with different cooling rates immersed in SBF for 72 h: (a) C1, (b) C2, (c) C3, (d) C4 and (e) C5.

3.3. Corrosion behaviour in immersion tests

Fig. 6 shows the corrosion rate variation as a function of cooling rate for the Mg–Zn–Ca alloys. It can be seen from the figure that the corrosion rate decreases with increasing cooling rate. This result suggests again that the corrosion resistance of the alloy was improved as cooling rate increased, which is inconsistent with the electrochemical EIS measurement results. The result also clearly shows that the corrosion rate decreased with increasing immersion time. It was observed that the corrosion rate was high in the first 12 hours and then gradually reached a stable stage upon further immersion. A possible explanation may be given in terms of the formation of a corrosion product layer. The corrosion products deposited on the sample surface developed into a continuous layer upon corrosion and thickened as the immersion test went on. The layer

could well play a protective film, retarding further degradation. Fig. 7 shows the surface morphologies of the Mg–2Zn–0.5Ca alloy solidified at different cooling rates and immersed in SBF for 72 h. It can be seen that the amount of corrosion products decreased with increasing cooling rate. On the other hand, corrosion pits were observed on the surface of the C1 sample solidified at the lowest cooling rate and the corrosion film was loose and porous. For the samples solidified at higher cooling rates, the corrosion film became more compact and corrosion became more homogeneous, indicating a change in corrosion mechanism from pitting to overall corrosion. All these observations verified the analysed results from both the electrochemical and immersion tests that increasing cooling rate improved the corrosion resistance of the material.

The change in corrosion mechanism from pitting to overall corrosion is important in corrosion control. High cooling rate

can lead to grain refinement, enhancing microstructural and chemical homogeneity, which can decrease activity and probability of local micro-galvanic corrosion and turn pitting corrosion into overall corrosion mechanism. Moreover, as shown in Figs. 2 and 3, the continuity of intergranular eutectic phase increased as the grain size reduced, which could play as a barrier to the corrosion of the alloy.

4. Conclusions

Microstructural evolution and corrosion behaviour in an Mg–2Zn–0.5Ca alloy solidified at different cooling rates were investigated in order to clarify the effect of rapid solidification on the corrosion resistance of the material. The conclusions obtained in this study are summarized as below:

- (1). Increasing solidification cooling rate resulted in a decrease in the average grain size and the secondary phase became more dispersive and continuous.
- (2). The corrosion resistance of the material improved with the increasing cooling rate, with apparently increased corrosion potential and homogenized corrosion mechanism.
- (3). The improvement in the corrosion behaviour is attributed to the cooling rate enhanced microstructural refinement, chemical homogeneity and solubility enhancement for the alloying element.

Acknowledgements

The authors are grateful for the supports from the National Natural Science Foundation of China (Nos. 51271131 and 51311130136).

References

- [1] Mark P. Staiger, Alexis M. Pietak, Jerawala Huadmai, George Dias, *Biomaterials* 27 (2006) 1728–1734.
- [2] Y.F. Zheng, X.N. Gu, F. Witte, *Mater. Sci. Eng. R* 77 (2014) 1–34.
- [3] Shaoxiang Zhang, Xiaonong Zhang, Changli Zhao, Jianan Li, Yang Song, Chaoying Xie, Hairong Tao, Yan Zhang, Yaohua He, Yao Jiang, Yujun Bian, *Acta Biomater.* 6 (2010) 626–640.
- [4] Jianan Li, Yang Song, Shaoxiang Zhang, Changli Zhao, Fan Zhang, Xiaonong Zhang, Lei Cao, Qiming Fan, Tingting Tang, *Biomaterials* 22 (2010) 5782–5788.
- [5] Xuenan Gu, Yufeng Zheng, Yan Cheng, Shengping Zhong, Tingfei Xi, *Biomaterials* 30 (2009) 484–498.
- [6] Zijian Li, Xunan Gu, Siquan Lou, Yufeng Zheng, *Biomaterials* 29 (2008) 1329–1344.
- [7] C.L. Liu, Y.J. Wang, R.C. Zeng, X.M. Zhang, W.J. Huang, P.K. Chu, *Corros. Sci.* 52 (10) (2010) 3341–3347.
- [8] M. Bobby Kannan, R.K. Singh Raman, *Biomaterials* 29 (2008) 2306–2314.
- [9] W.-C. Kim, J.-G. Kim, J.-Y. Lee, H.-K. Seok, *Mater. Lett.* 62 (2008) 4146–4148.
- [10] Hui Du, Zunjie Wei, Xinwang Liu, Erlin Zhang, *Mater. Chem. Phys.* 125 (2011) 568–575.
- [11] Y. Xia, B. Zhang, Y. Wang, M. Qian, L. Geng, *Mater. Sci. Eng. C* 32 (4) (2012) 665–669.
- [12] H.X. Wang, S.K. Guan, X. Wang, *Acta Biomater.* 6 (2010) 1743–1748.
- [13] B. Zhang, Y. Hou, X. Wang, Y. Wang, L. Geng, *Mater. Sci. Eng. C* 31 (2011) 1667–1673.
- [14] K.D. Ralston, N. Birbilis, *Effect of grain size on corrosion: a review*, *Corrosion* 66 (2010) 1–13.
- [15] G.R. Argade, S.K. Panigrahi, R.S. Mishra, *Corros. Sci.* 58 (2012) 145–151.
- [16] Jun Du, Minghua Wang, Mingchuan Zhou, Wenfang Li, *J. Alloys Compd.* 15 (2014) 313–318.
- [17] Srikant Gollapudi, *Corros. Sci.* 62 (2012) 90–94.
- [18] M. Alvarez-Lopez, Maria Dolores Pereda, J.A. del Valle, M. Fernandez-Lorenzo, M.C. Garcia-Alonso, O.A. Ruano, M.L. Escudero, *Acta Biomater.* 6 (2010) 1763–1771.
- [19] Fan Zhang, Aibin Ma, Jinghua Jiang, Honglu Xu, Dan Song, Fumin Lu, Yoshinori Nishida, *Prog. Nat. Sci. Mater. Int.* 23 (4) (2013) 420–424.
- [20] J.H. Gao, S.K. Guan, Z.W. Ren, Y.F. Sun, S.J. Zhu, B. Wang, *Mater. Lett.* 65 (2011) 691–693.
- [21] Michiaki Yamasaki, Naoyuki Hayashi, Shogo Izumi, Yoshihito Kawamura, *Corros. Sci.* 49 (2007) 255–262.
- [22] Michiaki Yamasaki, Shogo Izumi, Yoshihito Kawamura, Hiroki Habazaki, *Appl. Surf. Sci.* 19 (2011) 8258–8267.
- [23] Shogo Izumi, Michiaki Yamasaki, Yoshihito Kawamura, *Corros. Sci.* 51 (2009) 395–402.
- [24] Jing-feng Wang, Song Huang, Sheng-feng Guo, Yi-yun Wei, Fu-sheng Pan, *Trans. Nonferr. Met. Soc. China* 23 (2013) 1930–1935.
- [25] Hiren R. Kotadia, Ph.D. Brunel University, UK, 2010.
- [26] American Society for Testing and Materials, ASTM-G31-72, American Society for Testing and Materials, Philadelphia, PA, 2004.
- [27] P.M. Jardim, G. Solórzano, J.B. Vander Sande, *Mater. Sci. Eng. A* 381 (2004) 196–205.
- [28] Dong-song Yin, Er-lin Zhang, Song-yan Zeng, *Trans. Nonferr. Met. Soc. China* 4 (2008) 763–768.